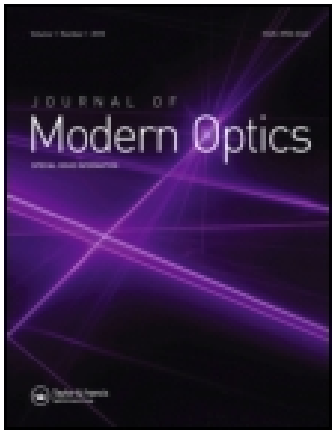

Journal of Modern Optics
Publication details, including instructions for authors and subscription information:
http://www.tandfonline.com/loi/tmop20

Measurement of correlation between transmission and scattering during wound healing in hen corneas

S. Mar [a b], M.C. Martínez-García [c], T. Blanco-Mezquita [b], R.M. Torres [b] & J. Merayo-Lloves [b]

[a] Departamento de Física Teórica, Atómica y Óptica, Facultad de Ciencias, Universidad de Valladolid, Prado de la Magdalena s/n 47005, Valladolid, Spain

[b] Instituto de Oftalmobiología Aplicada, Facultad de Medicina, Universidad de Valladolid, Ramón y Cajal 7, 47005, Valladolid, Spain

[c] Departamento de Biología Celular e Histología, Facultad de Medicina, Universidad de Valladolid, Ramón y Cajal 7, 47005, Valladolid, Spain

Published online: 18 May 2009.

To cite this article: S. Mar, M.C. Martínez-García, T. Blanco-Mezquita, R.M. Torres & J. Merayo-Lloves (2009) Measurement of correlation between transmission and scattering during wound healing in hen corneas, Journal of Modern Optics, 56:8, 1014-1021, DOI: 10.1080/09500340902871389

To link to this article: http://dx.doi.org/10.1080/09500340902871389

Journal of Modern Optics
Vol. 56, No. 8, 10 May 2009, 1014–1021

Taylor & Francis
Taylor & Francis Group

Measurement of correlation between transmission and scattering during wound healing in hen corneas

S. Mar[a,b]*, M.C. Martínez-García[c], T. Blanco-Mezquita[b], R.M. Torres[b] and J. Merayo-Lloves[b]

[a]*Departamento de Física Teórica, Atómica y Óptica, Facultad de Ciencias, Universidad de Valladolid, Prado de la Magdalena s/n 47005, Valladolid, Spain;* [b]*Instituto de Oftalmobiología Aplicada, Facultad de Medicina, Universidad de Valladolid, Ramón y Cajal 7, 47005, Valladolid, Spain;* [c]*Departamento de Biología Celular e Histología, Facultad de Medicina, Universidad de Valladolid, Ramón y Cajal 7, 47005, Valladolid, Spain*

(*Received 13 November 2008; final version received 5 March 2009*)

The aim of this work is to provide experimental data for corneal transparency and scattering to help create a more complete model of corneal transparency. The scattered light in 96 healing hen corneas was measured for three wavelengths by a scatterometer constructed in the Optics Laboratory (The University of Valladolid, Spain). With the help of mirrors and beamsplitters, the light from the three lasers is directed toward the cell containing the sample to be measured. The measured scattered light varies between six orders of magnitude. Corneal transmissivity, mean cosine of a scattering angle, and angular distribution of scattered light were all computed. The total transmitted light remained practically constant over a wide range of light values transmitted in a forward direction (direct transmissivity). The value of the mean cosine of the scattering direction is very close to the unit ($g > 0.98$), even in corneas with high opacities. The behavior of g indicates that even damaged corneas evidence extremely small scattering, compared to other biological tissues. The transmission reduction of each cornea is related to an increase in scattered light. In all cases, scattered light is concentrated at very small angles. This behavior is acceptable in corneas that are healthy or which evidence small lesions, but remains in corneas that are severely injured.

Keywords: scattering; optical parameters; cornea; wound healing; hens

1. Introduction

There are various models to explain corneal transparency. The small amount of scattered light produced by this tissue has in particular been extensively researched in the literature [1–20]. All previous theories explaining corneal transparency [21–27] have focused on light propagation in the stromal extracellular matrix.

According to Benedek [21], light is scattered by way of fluctuations in the index of refraction. The size of these fluctuations must be greater than a half-wavelength of the light in the medium. They can be caused by microstructural alterations, the irregular organization of the extracellular matrix, or by cells [22]. Many studies have attempted to relate form, density, and cell size to the structure of the scattered light [1–7,17,18]. Mourant et al. [12,13] suggest that the cell itself is responsible for scattering at a small angle. At slightly larger angles, their data indicate that the nucleus is primarily responsible for scattering. Smaller organelles, such as mitochondria and endoplasmic reticulum, are likely responsible for scattering at larger angles. Møller-Pedersen [10,11] studied these particular unclear aspects. McCally et al. [8] presented the first measurements of light-scattering and their link to the ultrastructure of scars. For a more comprehensive study, see the reviews by Farrell and McCally [28] as well as Freegard [29].

All of these models were developed and tested in different types of tissues. However, the cornea has a special structure appropriate for light transmission. Previous studies have shown that scattering in a damaged cornea originates from microstructural alterations in the stromal extracellular matrix [8], as well as different cells such as keratocytes, fibroblasts, or myofibroblasts, or even certain elements of these cells [4,12,13]. When the healing process is complete, the stromal extracellular matrix recovers its order partially or entirely [30–32]. Cells become quiescent, alter their composition, reduce in number and size of organelles, and acquire a refractive index similar to the medium in order to prevent scattering.

Despite all the work conducted, there is still no reliable model that elucidates corneal transparency. The aim of this work is to provide experimental data for corneal transparency and scattering in order help create a more complete model of corneal transparency.

*Corresponding author. Email: santiago@opt.uva.es

ISSN 0950–0340 print/ISSN 1362–3044 online

DOI: 10.1080/09500340902871389
http://www.informaworld.com

In the present work, we demonstrated that the total light transmitted (total transmissivity) remains nearly constant over a wide range of direct transmissivity (light transmitted in a forward direction). We found the value of the mean cosine of the scattering to be very close to the unit, even in corneas with high opacities. In any case, scattering concentrates the light on very small angles, as compared to scattering in other tissue types.

A reduction in the light transmitted with small scattering should not dramatically affect imaging quality [33,34]. Nevertheless, the logarithmic response of the retina and the specific illumination conditions that lead to such small scattering may cause significant visual deficiencies.

2. Materials and methods

2.1. Animals

We tried to obtain corneas at different stages of wound healing using several surgical techniques and post-operative treatments to study the common behavior of light passing through the corneas.

Ninety-six adult hens, *Gallus gallus domesticus* (2 kg weight) were used. The animals were handled in compliance with the guidelines of the ARVO Statement for the Use of Animals in Ophthalmic and Vision Research. The procedures were approved by the Animal Research Ethics Committee of the University of Valladolid.

Surgical data and methods have already been described in the literature [35,36], and here we only explain the details specific to the current experiment. Hens were anesthetized with an intramuscular injection of ketamine hydrochloride (37.5 mg kg^{-1}; Ketolar, Parke-Davis S.A., Barcelona, Spain) and xylazine hydrochloride (5 mg kg^{-1}; Rompun, Bayer AG, Leverkusen, Germany), followed by topical application of 0.5% tetracaine chlorhydrate and 1 mg of oxybuprocaine (Colircusí Anestésico Doble, Alcon Cusí, S.A., Barcelona, Spain). PRK or LASIK was performed in both eyes. Each eye was ablated using a 6.0 mm diameter optical zone and received −6.00 D of treatment (68 μm) using an Apex Plus excimer laser (Summit, Waltham, MA). All procedures were performed under an operating microscope.

The animals were divided into seven groups: Group 1:PRK, NO drug treatment (13 corneas); Group 2:PRK, treatment carboxymethylcellulose sodium 0.5%, topical administration drops (13 corneas); Group 3:PRK, treatment fluorometholone 0.1% (13 corneas); Group 4:LASIK, NO drug treatment (16 corneas); Group 5:LASIK, treatment carboxymethylcellulose sodium 0.5%, topical administration drops (15 corneas); Group 6:LASIK, treatment fluorometholone 0.1% (15 corneas); Group 7:NO surgery, NO treatment, control (11 corneas). Animals were sacrificed with an intravenous injection of 150 mg kg^{-1} ketamine hydrochloride while under general anesthesia. Animals were euthanized at two different time points: 30 and 60 days after surgery. Animals and treatments formed part of a wider study performed by our research group, in which the corneas were used elsewhere.

2.2. Scatterometer

The experimental setup was a scatterometer (Figure 1) constructed in the Optics Laboratory (The University of Valladolid, Spain). With the help of mirrors and beamsplitters, the light from the three lasers

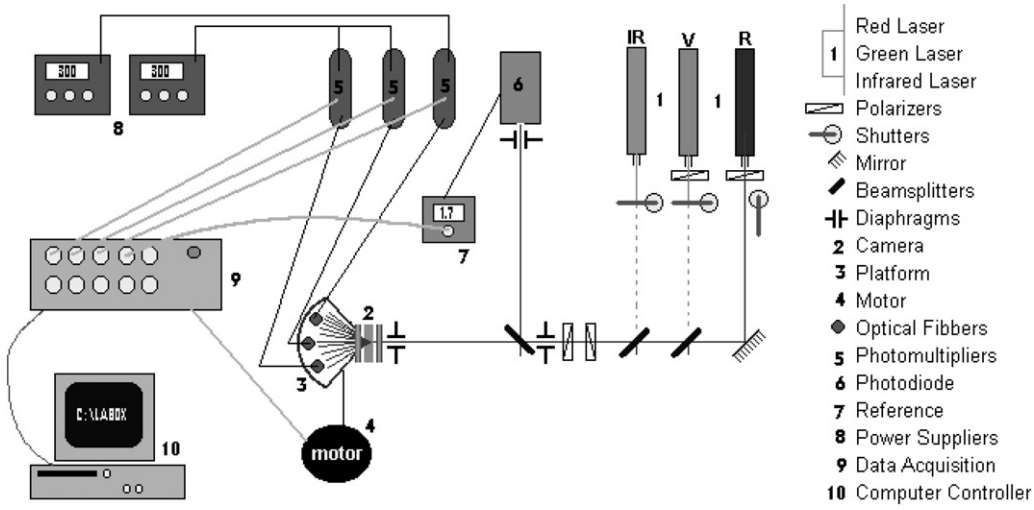

Figure 1. Experimental setup.

(Red He–Ne 632.8 nm, Green He–Ne 543.5 nm and infrared diode 830.0 nm) was directed toward the cell containing the sample to be measured. A set of polarizers controlled light intensity and defined the beam polarization plane, and a set of shutters enabled selection of probe wavelength.

Three optical fibers collected the light spread into the cell and sent it to individual photomultipliers (5). Fibers were placed on a platform (3) that rotates in a horizontal plane driven by a stepping motor (4). The platform's axis of rotation coincides with the impact point of the laser beam on the sample. Fibers were placed 44.5 mm from the axis of the rotation with an angle of 30° between them. With this arrangement, and assuming symmetric scattering [14,20], rotating the platform 30° enables the entire angular distribution of the scattered light to be obtained. However, the main reason for having three detection channels was the strong dependence of light intensity on the scattering angle. For this reason, each channel was programmed with a different sensitivity level depending on the measured angular interval. This procedure enabled the angular distribution of scattered light in a range greater than six orders of magnitude to be obtained. In order to control intensity variation of the laser radiation a fourth channel (6) collected part of the light emitted by the laser prior to it reaching the sample.

These corneas were placed on a stainless steel cell (2) which had a 26 mm diameter quartz window on both sides. These windows were 17 mm from each other. A liquid maintenance medium, with a constant temperature, flowed continuously through the cell.

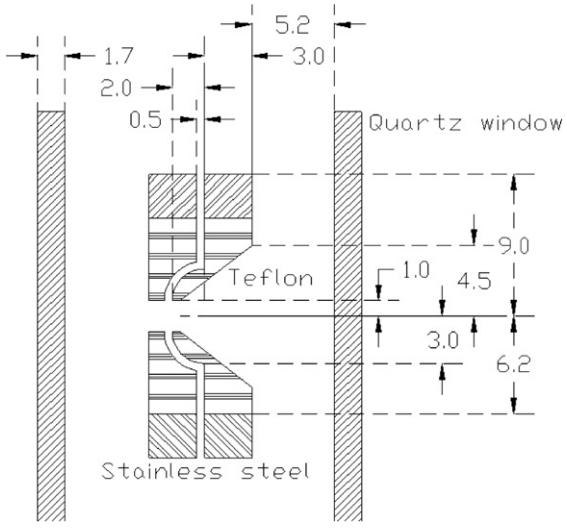

Figure 2. Horizontal section of the cornea holder. All data are in mm.

In order to place the cornea properly inside the cell, a device comprising two stainless steel sheets was used. The cornea was placed in a Teflon lodging between the two sheets, forming a 'sandwich'. The Teflon holder is made with a curvature that is similar to the cornea and has a 2 mm diameter hole, which is twice the diameter of laser in order to prevent any interference with the holder (Figure 2).

This arrangement does not limit the external measuring angle, which ranged from −85° to +85°, with respect to the incident beam. The main limitations are the geometry of the cornea-holder (Figure 2) and the critical angle of the second surface of the exit window ($n = 1.5118$). Depending on the refractive index of the immersion solution ($n = 1.3330$), the maximum scattering angle measured inside the cell was approximately 54°. However, the geometry of the cornea-holder limits this value to 38°. Henceforth, all scattering angles will refer to the inner part of the cell.

The entire system is computer (10) controlled: shutter opening, platform rotating, measure recording, etc. Measurement of the whole angular distribution of scattered light lasts only a few minutes in order to avoid corneal deterioration.

2.3. *Calibration of the scatterometer*

In order to test the experimental apparatus, a measurement of polymeric microsphere suspension (10% and 5%) in distilled water was carried out [17]. The nominal diameter of the microspheres was 3.063 (0.027) μm (Duke Scientific Corporation). The angular scattering distribution for each of the three lasers was measured. The behavior of the experimental setup is shown in Figure 3, which represents the angular

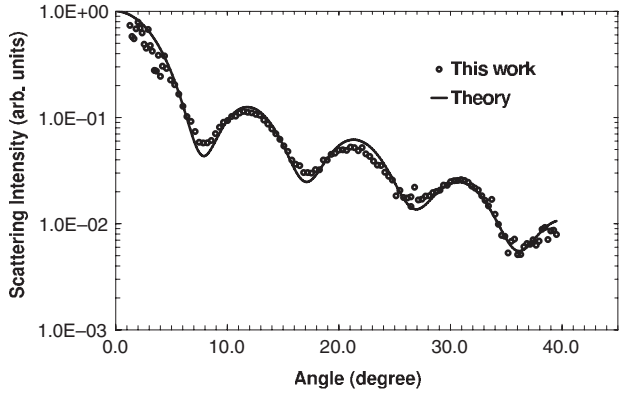

Figure 3. Scattering produced by a suspension of 5% of microspheres in distilled water. Dots: measurements carried out with the experimental setup shown in Figure 1. Line: behavior predicted by the Mie model (wavelength 632.8 nm).

distribution of scattered light for 5% suspension and a 632.8 nm wavelength. Along with the experimental data, predictions from a Mie model are shown. The Mie calculation was performed with the following data: sphere radius = 1.53 μm, refractive index of sphere = 1.59 + 0.0i, refractive index of water - 1.333 + 0.0i, wavelength = 0.6328 μm, size parameter = 20.25. In order to compare the numerical values calculated and the measured data, the maximum for both curves was normalized at the unit. For 10% suspension and a 543.5 nm wavelength, the behavior proved similar. The good agreement between the measured and calculated data in turn accounts for the reliability of the experimental arrangement.

The measurement protocol included recording the angular distribution of light intensity from the maintenance liquid without the cornea. These 'control' measurements were carried out every five or six measurements with the cornea, in which the angular resolution of the scatterometer was provided. The light intensity became half-maximum when the platform rotated $0.48^\circ \pm 0.01^\circ$ for the red laser, $0.48^\circ \pm 0.01^\circ$ for the green laser, and $0.47^\circ \pm 0.01^\circ$ for the infrared laser. It diminished at a factor of 10 when the platform rotated $0.79^\circ \pm 0.02^\circ$ for the red laser, $0.79^\circ \pm 0.02^\circ$ for the green laser, and $0.75^\circ \pm 0.01^\circ$ for the infrared laser. The angular resolution of the scatterometer is thus less than 1°.

These 'control' measurements also allow the accuracy of the transmissivity values to be calculated. Maximum light intensity in arbitrary units was 2.06 ± 0.20 for the red laser, 2.27 ± 0.20 for the green laser, and 2.06 ± 0.09 for the infrared laser. Experimental transmissivity values thus have an estimated uncertainty of around 10% after considering the different sources of experimental error.

Laser stability and fluctuation, measurement of shutter opening and closing times, and platform rotation angle were all previously carried out.

The polarization effect was also taken into account. Data were processed with routines developed by the authors. The code calculated the transmission factors of the boundary liquid-quartz and quartz-air (Fresnel's formulas). The measured data were calculated with the scattering intensities and angles inside the cell that were just behind the cornea. Henceforth, scattering intensity and angles will refer to the inner part of the cell.

The scatterometer was examined to ensure it had no detectable anisotropy. Several measurements with maintenance liquid (without the cornea) were performed for horizontal, vertical, and 45° polarizations, respectively. Results were indistinguishable within experimental error (10%).

2.4. Ex vivo *scattering measurements*

Using the previously described experimental setup, we measured the light transmission and scattering properties of 96 corneas: normal and surgical corneas after photorefractive keratectomy (PRK) and laser *in situ* keratomileusis (LASIK). The different treatments and surgical techniques have been described in detail in previous works [35–37], although some additional details concerning the present experiment will be provided here. The corneas ranged from healthy with close to 100% transmissivity to others that were nearly fully opacified, depending on the periods after surgery and treatments. Nevertheless, in this present work, we center on the correlation between transmissivity and scattering.

Once the cornea was removed from the animal, the surgeon carefully placed it in the cornea holder, attempting in turn to maintain it as stretched as possible. When the cornea holder was closed, the cornea conforms to this shape. The entire cornea was placed in the cell filled with maintenance liquid at a constant temperature and continuous flow. The refractive index of liquid (1.333) is very close to that of the cornea, helping in turn to eliminate any scatter from the liquid–cornea interface, irregularities of the corneal surface, and reduction of light convergence by the cornea. However, the cell used in this experiment produced no pressure difference between both sides of the cornea. Furthermore, a removed cornea tends to lose its tension. All of these effects cause problems in the light transmission measurement. Special care was thus taken when placing the cornea on its holder so as to ensure there were no wrinkles. As indicated above, when the cornea holder is closed, the cornea conforms to the shape of the holder (see Figure 2), similar to the original cornea shape, which is why transmission measurements were very close to cornea transmission before removal. Special care was also taken to prevent the formation of small bubbles adhering to the cornea.

The experiment optimized the reduction of time needed for *ex vivo* measurements and thus avoided tissue transparency loss. Total measurement time for each cornea was approximately 15 min although control experiments showed that tissue transparency remained unchanged even after one hour.

Corneal scattering was also seen to evidence rotational symmetry centered on the optical axis [38], [39]. This was examined by comparing several measurements, rotating the cornea, and the polarization of the incident light. Results obtained were identical to experimental errors. For this reason, vertical polarization was always used and angular scanning was performed on the horizontal plane. To calculate the

integral magnitudes we used the rotational symmetry properties of the scattered light.

3. Results

For each cornea, measurements were taken for 146 angular positions ranging from -1.2° to $+85^\circ$ outside the cornea cell, corresponding to the -0.9° and 48.6° inner part of the cell.

Data processing provided the following magnitudes for every wavelength:

(a) angular distribution of the scattered light;
(b) mean cosine of the scattering angle, g;
(c) transmission in a forward direction, which will be referred to as direct transmissivity;
(d) ratio between total transmitted energy integrated for all angular positions and total incident energy, which will be referred to as total transmissivity;
(e) the half-width of the angular distribution of the scattered light for intensities corresponding to 1/2, 1/10, 1/100, 1/1000, 1/10,000, and 1/100,000 of maximum intensity.

3.1. Correlation of total transmissivity to direct transmissivity

Figure 4 shows total transmissivity versus direct transmissivity for all the corneas. Total transmissivity showed significant data dispersion, partly due to the experimental error of the measurement. Angular intensities that contributed most to the final total transmissivity value corresponded to large angles, which unfortunately have larger errors.

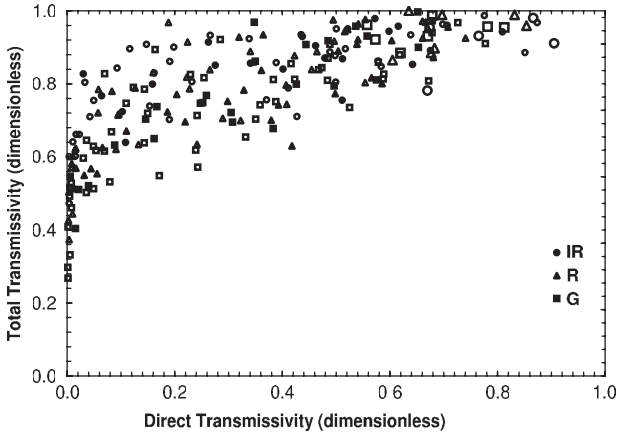

Figure 4. Total transmissivity versus direct transmissivity for each cornea and wavelength. IR: infrared 830 nm, R: red 633 nm, G: green 543 nm. Large symbols; control corneas, small symbols; operated corneas, closed symbols; untreated corneas, and open symbols; treated corneas.

If corneas with very high opacities are not taken into account (direct transmissivity $< 1\%$), average direct transmissivity values are: 0.40 ± 0.25 for the red laser, 0.38 ± 0.23 for the green laser, 0.46 ± 0.26 for the infrared laser, and 0.41 ± 0.25 for all lasers. Average total transmissivity values are: 0.86 ± 0.17 for the red laser, 0.85 ± 0.17 for the green laser, 0.93 ± 0.16 for the infrared laser, and 0.88 ± 0.17 for all lasers.

Despite data dispersion, total transmissivity value remains almost constant at approximately 88% for all the wavelengths used as well as for both treated and normal corneas. A slight increase was observed with direct transmissivity, except for corneas whose direct transmissivity was below 10%.

3.2. The mean cosine of the scattering angle

The measured scattering angular distribution $I(\theta)$ of a cornea with 22% transmissivity can be seen in Figure 5. When assuming single scattering, it is possible to calculate the mean cosine of a scattering angle, g, from the angular intensity measurement $I(\theta)$ via:

$$g = \frac{\int_{4\pi} \cos\theta \times I(\theta) \times \mathrm{d}\omega}{\int_{4\pi} I(\theta) \times \mathrm{d}\omega},$$

where θ is the scattering angle and $\mathrm{d}\omega$ the solid angle.

The mean cosine of the scattering angle (g) versus direct transmissivity is shown in Figure 6. Except for corneas with very severe opacities (direct transmissivity $< 10\%$), the value of g is very close to the unit ($g > 0.99$). This value is acceptable in healthy corneas, since scattering is very small. However, in most tissues [40] g is usually between 0.6 and 0.9. This behavior of g indicates that even damaged corneas present very small scattering compared to other biological tissues. In order to lose these properties, very severe opacity must be present, allowing transmissivity below 10%.

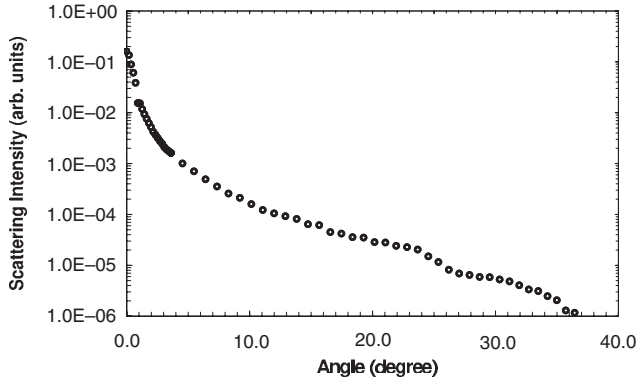

Figure 5. Scattering angular distribution for a cornea with 22% transmissivity.

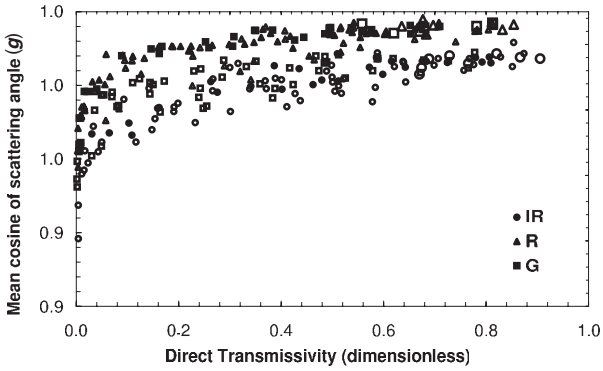

Figure 6. Mean cosine of scattering angle (g) versus direct transmissivity. IR: infrared 830 nm, R: red 633 nm, G: green 543 nm. Large symbols; control corneas, small symbols; operated corneas, closed symbols; untreated corneas, and open symbols; treated corneas.

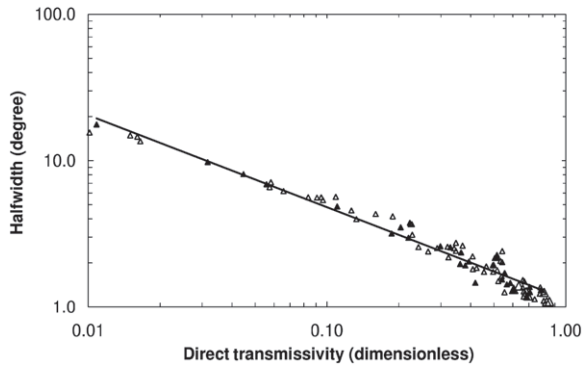

Figure 7. The half-width of the scattering angular distribution for intensities corresponding to 1/100 of the maximum intensity versus direct transmissivity. Large symbols; control corneas, small symbols; operated corneas, closed symbols; untreated corneas, and open symbols; treated corneas.

3.3. The scattering angular distribution

Figure 7 shows the half-width of the scattering angular distribution for intensities corresponding to 1/100 of the maximum intensity for the red wavelengths. Angular width is expressed in degrees. The lower the direct transmissivity the greater the angular distribution and width. There is a correlation (log–log) between scattering width and direct transmissivity. However, this correlation disappears in the tails of the scattering curve (intensities below 1/100 of the maximum). The same behavior was observed for all the different wavelengths.

4. Discussion

The avian cornea consists of five layers: epithelium, Bowman's layer, stroma, descemet layer, and endothelium. The vast majority of corneal thickness (90%) is stroma, which is made up of collagen fibrils in layers or 'lamellae' in the plane of the cornea and keratocytes [41]. The difference between human and avian corneas is the orientation of the grids at different successive levels [42] and the bilateral asymmetry [43,44].

During corneal wound healing, the natural conformation of the extracellular matrix is altered, along with changes in cellular density and phenotype, linked to the production of disorganized extracellular matrix components. The result is a decrease in transmission and an increase in scattering.

Despite data dispersion, we found that total transmissivity is approximately 88%. This result confirms that absorption, backscattering (haze), and reflection are small, approximately 12%. This was known in healthy as well as slightly injured corneas [28,29]. Moreover, this result is extended to corneas with severe opacities.

This finding is compatible with other experimental data. Jester et al. [4] measured reflection and backscattering and found a remarkable increase in damaged regions with a high density of keratocytes. This behavior is interpreted as the lack of protein ALDH3 in the keratocytes and the consequent reduction in homogeneity in the refractive index of corneas. Indeed, as direct transmissivity decreases there is a small reduction in total transmitted energy, which is compatible with the increase in backscattering.

As McCally et al. [8] show, direct transmissivity depends on the structure organization of the tissue. Furthermore, the shape of the central part of the scattering curve is related to the types of cells that make up the corneal tissue [12]. This is different for each cornea, depending on the course of the healing. Therefore, the scattering curve and transmission are not necessarily related. Obviously, the greater the corneal wound the more disorganized the tissue, and there are also a larger number of elements that contribute to scattering. For this reason, there is always a correlation between scattering widths and transmission.

An increase in the scattering angular width implies a decrease in contrast sensitivity. As shown in this work (Figures 4 and 6) most of the scattered light comprises small angles. The mean cosine value of scattering is very close to the unit even in seriously damaged corneas. However, absorption, reflection or backscattering would have no significant impact on the quality of the retinal image. It might then be posited that a reduction in contrast sensitivity should not appear in this type of corneal lesion and that the information given by scattered light for large angles should prove irrelevant. However, the retina's sensitivity is logarithmic, which implies that very low intensities can be

detected if ground illumination is low. These conditions are broken when outer illumination is extremely low and there is an intense luminous point, in which case the information given by scattered light for large angles does prove relevant.

In conclusion, direct transmissivity reduction of each cornea is related to an increase in scattered light, which might be due to the damaged tissue's lack of structure or to the cells that appear in the healing process. In any case, scattering concentrates the light on very small angles, as compared to scattering in other types of tissues. This behavior is reasonable in corneas that are healthy or present minor lesions, but remains in corneas that are severely injured. In our opinion, this allows corneas with high opacities to maintain a certain capacity to form images in the retina.

Acknowledgements

We would like to thank Dr J.A. Aparicio, V.R. Gonzalez, G. Rodriguez, S. Najera, and S. Gonzalez for their collaboration. This work was supported in part by grant FIS-PI:01/0270 and Red Temática de Investigación Cooperativa en Oftalmología CO3/13, Instituto de Salud Carlos III, Ministerio de Sanidad y Consumo, Madrid, Spain. Alcon-Cusi SA (Barcelona, Spain) donated the experimental excimer laser.

References

[1] Braunstein, R.E.; Jain, S.; McCally, R.L.; Stark, W.J.; Connolly, P.J.; Azar, D.T. *Ophthalmology*. **1996,** *103,* 439–533.
[2] Chan, W.W.; Edwards, M.H.; Woo, G.C.; Woo, V.C.P *J. Cataract Refract. Surg*. **2003,** *29,* 118–124.
[3] Drezek, R.; Dunn, A.; Richards-Kortum, R. *Appl. Opt*. **1999,** *38,* 3651–3661.
[4] Jester, J.V.; Møller-Pedersen, T.; Huang, J.; Sax, C.M.; Kays, W.T.; Cavangh, H.D.; Petroll, W.M.; Piatigorsky, J. *J. Cell Sci*. **1999,** *112,* 613–622.
[5] Lohmann, C.P.; Gartry, D.S.; Kerr-Muir, M.; Timberlake, G.T.; Fitzke, F.W.; Marshall, J. *Eur. J. Ophthalmol*. **1991,** *1,* 173–180.
[6] Lohmann, C.P.; Timberlake, G.T.; Fitzke, F.W.; Gartry, D.S.; Kerr-Muir, M.; Marshall, J. *Refract. Corneal Surg*. **1992,** *8,* 114–121.
[7] McCally, R.L.; Connolly, P.J.; Jain, S.; Azar, D.T. *Ophthalmic Technol. IV*. **1994,** *2126,* 161–165.
[8] McCally, R.L.; Freund, D.E.; Zorn, A.; Bonney-Ray, J.; Grebe de la, R.; Cruz, Z.; Green, W.R. *Investigat. Ophthalmol. Vis. Sci*. **2007,** *48,* 157–165.
[9] Meek, K.M.; Leonard, D.W.; Connon, C.J.; Dennis, S.; Khan, S. *Eye*. **2003,** *17,* 927–936.
[10] Møller-Pedersen, T. *Acta Ophthal. Scandinav*. **2003,** *81,* 6–20.
[11] Møller-Pedersen, T. *Exper. Eye Res*. **2004,** *78,* 553–560.
[12] Mourant, J.R.; Freyer, J.P.; Hielscher, A.H.; Eick, A.A.; Shen, D.; Johnson, T.M. *Appl. Opt*. **1998,** *37,* 3586–3593.
[13] Mourant, J.R.; Canpolat, M.; Brocker, C.; Esponda-Ramos, O.; Johnson, T.M.; Matanock, A.; Stetter, K.; Freyer, J.P. *J. Biomed. Opt*. **2000,** *5,* 131–137.
[14] Mourant, J.R.; Johnson, T.M.; Doddi, V.; Freyer, J.P. *J. Biomed. Opt*. **2002,** *7,* 93–99.
[15] Drezek, R.; Guillaud, M.; Collier, T.; Boiko, I.; Malpica, A.; Macaulay, C.; Follen, M.; Richars-Kortum, R. *J. Biomed. Opt*. **2003,** *8,* 7–16.
[16] Ramachandran, J.; Powers, T.M.; Carpenter, S.; Garcia-Lopez, A.; Freyer, J.P.; Mourant, J.R. *Opt. Express*. **2007,** *15,* 4039–4053.
[17] Soya, K.; Amano, S.; Oshika, T. *Ophthalmic Res*. **2002,** *34,* 380–388.
[18] Van den Berg, T.J.TP *Invest. Ophthalmol. Vis. Sci*. **1997,** *38,* 1321–1332.
[19] Wilson, J.D.; Foster, T.H. *Opt. Lett*. **2005,** *30,* 2442–2444.
[20] Wilson, J.D.; Cottrell, W.J.; Foster, T.H. *J. Biomed. Opt*. **2007,** *21,* 014010:1–10.
[21] Benedek, G.B. *Appl. Opt*. **1971,** *10,* 459–473.
[22] Connon, C.J.; Meek, K.M.; Kinosshita, S.; Quantock, A.J. *Exper. Eye Res*. **2004,** *78,* 909–915.
[23] Farrell, R.A.; McCally, R.L.; Tatham, P.E. *J. Physiol. Lond*. **1973,** *233,* 589–612.
[24] Goldman, J.N.; Benedek, G.B. *Invest. Ophthalmol*. **1967,** *6,* 574–600.
[25] Goldman, J.N.; Benedek, G.B.; Dohlman, C.H.; Kravitt, B. *Invest. Ophthalmol*. **1968,** *7,* 501–519.
[26] Hart, R.W.; Farrell, R.A. *J. Opt. Soc. Am*. **1969,** *59,* 766–774.
[27] Maurice, D.M. *J. Physiol. Lond*. **1957,** *136,* 263–286.
[28] Farrell, R.A.; McCally, R.L. Corneal Transparency. In *Principles and Practice of Ophthalmology*, 2nd ed.; Albert, D.M., Jakobiec, F.A., Eds.; WB Saunders: Philadelphia, 2000; pp 629–644.
[29] Freegard, T.J. *Eye*. **1997,** *11,* 465–471.
[30] Aghamohammadzadeh, H.; Newton, R.H.; Meek, K.M. *Structure*. **2004,** *12,* 249–256.
[31] Chang, S.W.; Benson, A.; Azar, D.T. *J. Cataract Refract. Surg*. **1998,** *24,* 1064–1069.
[32] Zickler, M.H.L; Giese, G.; Walter, M.; Loesel, F.H.; Bille, J.F. *J. Biomed. Opt*. **2004,** *9,* 760–766.
[33] Van de Pol, C.; Soya, K.; Hwang, D.G. *Am. J. Ophthalmol*. **2001,** *132,* 204–210.
[34] Van den Berg, T.J.TP *J. Biomed. Opt*. **1996,** *1,* 262–267.
[35] Martinez-Garcia, C.; Merayo-Lloves, J.; Blanco-Mezquita, T.; Mar-Sardana, S. *Exper. Eye Res*. **2006,** *83,* 728–735.
[36] Torres, R.M.; Merayo-Lloves, J.; Blanco-Mezquita, J.T.; Gnther, C.P.; Rodriguez, G.; Gutierrez, R.; Martínez-García, C. *J. Refract. Surg*. **2005,** *21,* 392–398.
[37] del Val, J.A.; Barrero, S.M.; Yáñez, B.; Merayo, J.; Aparicio, J.A.; González, V.R.; Pastor, J.C.; Mar, S. *Appl. Opt*. **2001,** *40,* 1727–1734.
[38] McCally, R.L.; Farrel, R.A. *J. Refract. Surg*. **1999,** *15,* 706–710.

[39] Christens-Barry, W.A.; Green, W.J.; Connolly, P.J.; Farrell, R.A.; McCally, R.L. *Exper. Eye Res.* **1996,** *62,* 651–662.
[40] Vitkin, I.A.; Woolsey, J.; Wilson, B.C.; Rox Anderson, R. *Photochem. Photobiol.* **1994,** *59,* 455–462.
[41] Birk, D.E.; Fitch, J.M.; Babiarz, J.P.; Doane, K.J.; Linsenmayer, T.F. *J. Cell Sci.* **1990,** *95,* 649–657.
[42] Coulombre, A.J.; Coulombre, J.L. The Development of the Structural and optical Properties of the Cornea. In *The Structure of the Eye*: Smelser, G., Ed.; Academic Press: New York, 1961; pp 405–420.
[43] Meek, K.M.; Fullwood, N.J. *Micron.* **2001,** *32,* 261–272.
[44] Trelstad, R.L. *Dev. Biol.* **1982,** *92,* 133–134.